Hydrometallurgy 185 (2019) 266–272

Contents lists available at ScienceDirect

Hydrometallurgy

journal homepage: www.elsevier.com/locate/hydromet

Selective silica gel free scandium extraction from Iron-depleted red mud slags by dry digestion

Gözde Alkan[a,*,1], Bengi Yagmurlu[a,b,1], Lars Gronen[c], Carsten Dittrich[b], Yiqian Ma[a], Srecko Stopic[a], Bernd Friedrich[a]

[a] IME - Process Metallurgy and Metal Recycling, RWTH Aachen University, Aachen, Germany
[b] MEAB Chemie Technik GmbH, Aachen, Germany
[c] IML - Chair of Applied Mineralogy and Economic Geology, RWTH Aachen University, Aachen, Germany

ABSTRACT

A combination of pyrometallurgical and hydrometallurgical processes showed promising results for the sustainable valorisation of red mud with selective iron recovery. However; high Si content in red mud and its slags produced by pyrometallurgical treatment for the Fe removal makes these secondary resources untreatable with conventional acid leaching routes due to the formation of silica gel. In this study, red mud and slags synthesized by electric arc furnace smelting, which contain both moderate and extensive SiO_2, were exposed to dry digestion aiming selective Sc recovery with suppressed Ti and Si dissolution. Various additions of concentrated sulfuric acid were investigated to find out the optimum acid consumption for this process. A promising Sc leaching efficiency was found for acidic slag (~80%), where Ti dissolution was suppressed to < 10% and without Si gel formation. The mineralogical content of red mud and the two slags were analysed by QEMSCAN and XRD in order to elucidate the leaching mechanism. Using the findings of this study, an empirical dry digestion leaching model was proposed for each starting material in a comparative manner.

1. Introduction

Scandium (Sc), which is considered as one of the most promising candidates for future transportation and energy industry owing to its unique behaviours in both light weight alloys and Zr based solid oxide fuel cells, is an expensive metal due to inadequate primary sources, complex extraction and production routes (Marquis and Seidman, 2001; Røyset and Ryum, 2005; Yamamoto, 2000). Thus, this metal has already been classified as one of the critical metals for future in European Commission (Commission, 2017). Traditionally, Sc is produced from by-products of uranium, titanium pigment and nickel laterite processing (Feuling, 1991; Haslam, 1999; Kaya et al., 2017). Another promising and superior Sc secondary resource is bauxite residue (red mud), which is the main waste product of Bayer process. Many efforts have been made to extract and separate a Sc product from red mud in the last decades; however, non-selective metal mobilization, especially Fe and Ti, results in increasing complexity of purification and precipitation process of Sc (Alkan et al., 2017b; Alkan et al., 2018; Avdibegović et al., 2018; Borra et al., 2015; Narayanan et al., 2017; Paramguru et al., 2004; Yagmurlu et al., 2017). Hence, the utilization of red mud slags from which Fe has been removed pyrometallugically and with enriched Sc content is the focus of this study. It is possible to smelt red mud via Electric Arc Furnace (EAF) by recovering pig iron wih 95% efficiency and yield in a slag enriched in terms of Sc, Ti and REE, whose crystallinity and chemistry can be controlled by fluxing agents and cooling rates. Nevertheless, electric arc furnace (EAF) treated slags with depleted Fe content are also enriched in terms of SiO_2 content, especially for the cases where SiO_2 is used as flux during pyrometallurgical treatment. This causes significant processing difficulties for the direct acidic leaching which would magnify the common Si-gelation problem (Queneau and Berthold, 1986).

Dry digestion, which is defined as a process consisting of the addition of a concentrated acid to the solid materials with subsequent water leaching, is reported as an effective method against silica gel formation. The principle of dry digestion method is very similar to acid-baking technique, which was utilized to form water soluble sulphates from complex ore concentrates such as enargite and monazite, by concentrated sulfuric acid at a temperature range of 160-280 °C(Sadri et al., 2017; Safarzadeh et al., 2012a; Safarzadeh et al., 2012b). Dry digestion process, similarly applying concentrated acid but at lower temperatures (< 100 °C), was first defined in our previous study by Voßenkaul et al., where eudialyte ores were subjected to concentrated HCl to recover rare earth elements(Voßenkaul et al., 2017). 93% of REE recovery and inhibited silica gel formation was reported. It was also shown

* Corresponding author.
E-mail address: galkan@ime-aachen.de (G. Alkan).
[1] These authors contributed equally to this work.

https://doi.org/10.1016/j.hydromet.2019.03.008
Received 16 January 2019; Received in revised form 1 March 2019; Accepted 17 March 2019
Available online 19 March 2019

previously that successful recovery of Nb, Zr and Hf from eudialyte by dry digestion followed by oxidative water leaching was achieved (Ma et al., 2018). In another study by Rivera et al. (2018), this technique was applied on bauxite residue with the aim of REE and Sc recovery, where promising REE and Sc leaching efficiencies were reported.

In this study, it is aimed to apply dry digestion on EAF treated slags of red mud which is depleted in Fe but relatively enriched in Si. We aim to enhance Sc leaching efficiency and selectivity and examine the strength of dry digestion techniques on high Si content slags. One acidic (SiO_2 as flux during the smelting), one basic (CaO as flux) and untreated red mud as reference sample were exposed to dry digestion with concentrated H_2SO_4. Varying amounts of acid were examined to determine the optimum leaching condition. Inductively coupled plasma (ICP) was used to calculate leaching efficiencies of the focused elements, Sc, Ti and Si. X-ray diffraction (XRD), scanning electron microscopy (SEM) and Quantitative Evaluation of Minerals by Scanning Electron Microscopy (QEMSCAN) were utilized to understand the mineralogy and microstructure of starting slags and leach residues. By this comparative parametric study, the most promising pyrometallurgy-hydrometallurgy combination route for highest and the most selective Sc leaching with suppressed silica gelation were investigated and explained on the basis of slag characteristics. The operational flow diagram and the steps followed are presented in Fig. 1.

2. Experimental procedure

The bauxite residue (BR) from Aluminum of Greece and two different electrical arc furnace treated slags were used in this study. BR dry powder was consecutively mixed with lignite coke and lime containing 87 wt% fixed carbon and 95 wt% CaO and 98 wt% SiO_2, respectively. The additions of lignite coke and total flux to BR were 1:10 and 1:5, respectively. Flux additions of 100% lime and 100% silica were used for making basic and acidic slag; respectively. Batch masses of 1.5 kg of the aforementioned recipes were fed into a 100 KVA DC electric arc furnace. The material was contained in a graphite crucible, and the smelting was undertaken at temperatures in the range between 1500 and 1550 °C for one hour. At the end of the experiment, the melt was cast into a refractory-lined mould where the melt cooled down under ambient conditions and the metal settled at the bottom of the mould. The cooled material was manually separated into slag and metal and then weighed. The slag was prepared for leaching by crushing and milling to obtain a slag fraction of −90 μm.

Chemical composition of three starting solid materials are listed in Table 1 evaluated by ICP-OES measurement.

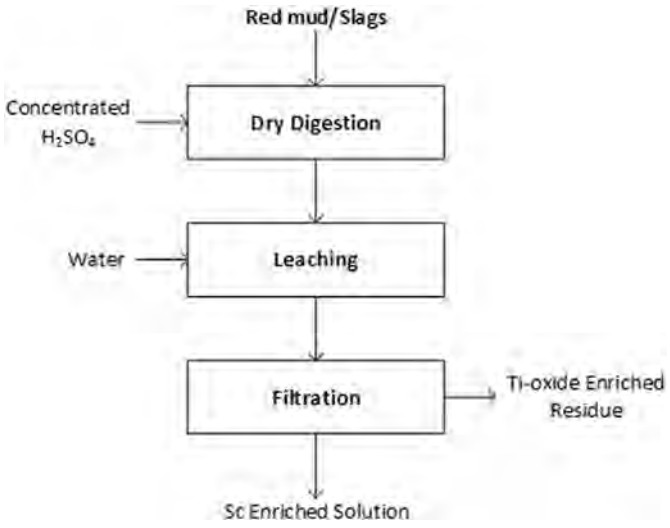

Fig. 1. Flow diagram if dry digestion procedure.

Table 1
Chemical composition of bauxite residue and EAF treated slag.

wt%	Fe_2O_3	Al_2O_3	CaO	SiO_2	TiO_2	Sc (mg/kg)
Bauxite residue	43.5	24	10.2	5.5	5.6	130
Basic slag	1.8	38.3	43.2	7.6	7.6	170
Acidic slag	1.4	36.8	15.3	38	7.3	170

All three solid residues were treated by direct leaching and by dry digestion to observe and compare the differences of these operations. In the direct leaching tests, a glass beaker, a heating plate, and a magnetic stirrer were used for controlling the reaction temperature and stirring speed. Starting solid materials were added into the reactor, containing the pre-heated sulfuric acid 2.5 M (H_2SO_4) solution. Leaching efficiency was investigated at a set temperature of 75 °C, 250 rpm stirring speed, and S/L ratio of 1/10 for 1 h.

Dry digestion process was performed with concentrated 97 wt% (H_2SO_4). Concentrated sulfuric acid is introduced to red mud and slags to form a paste and ensure silica precipitation. The absence of free water results in an extreme ionic strength avoiding chain formation of a gel. 13 g of starting materials were mixed manually for 5 min with various amounts of acid (5, 10, 15, ml) and in each case 5 ml DI water. In dry digestion, a certain amount of water is needed to ensure complete wetting, ionization of acid and diffusion [ref] After that the pastes were kept constant at 75 °C oven for 1 h. Afterwards, the paste is poured into DI water and stirred magnetically at room temperature for half an hour to solve precipitated sulphates in water and collect metals in the solution, this step is also named as washing.

Leachates were analysed with ICP OES technique to obtain leaching efficiencies. Solid samples were analysed by QEMSCAN and XRD. For QEMSCAN® analysis, the acceleration voltage was set to 25 kV. The sample current was set to 10 nA at an working distance of 13 mm. The point spacing was set to 7.5 μm per step and 2000 X-ray counts were recorded per step. Phase interpretation and further image analysis, like phase map, modal composition and elemental mapping, were performed by using iDiscover software suite (FEI).

XRD analyses was performed by Bruker D8 Advanced Diffractometer, which use Bragg- Brentano Geometry and θ- θ synchronization for X-Ray tube and the detector. 10°-80° (2 θ) were scanned with a 5° /min rate. The generator voltage was 40 kV and current was 40 nA. The quantitative evaluation was carried out with the program Topas (Bruker, AXS). For Rietveld analysis, the full profile method was used 0-point errors, specimen height errors, diffraction-peak intensities, LP-factor, background and crystal structure models were refined.

Particle size distribution was obtained using QEMSCAN© based image analysis. Thereby, multi-phase particles where extracted virtually from the recoded field images. Before analysis particles < 10 μm were filtered out to avoid misinterpretations. The generated particle population was analysed for their size distribution by the use of equivalent sphere diameter (ESD) method according to Heilbronner and Barrett (2014).

3. Results and discussion

XRD analyses given in Fig. 2, was utilized to reveal the starting phase composition of two slags and red mud in a comparative manner.

XRD analyses revealed that by EAF treatment, a dramatic change of phase content was occurred in both acidic and basic slags. Hematite is the most dominant phase of red mud accompanied by goethite, boehmite, diaspore, gibbsite and other silicates and via depletion of iron this was replaced by Ca, Al, Si mixed oxides in both slags. Moreover, the two slags between each other also exhibit different characteristics which may in turn affect leaching behaviour. The most apparent difference is observed in the crystallinity. Well defined and narrow peaks of the basic

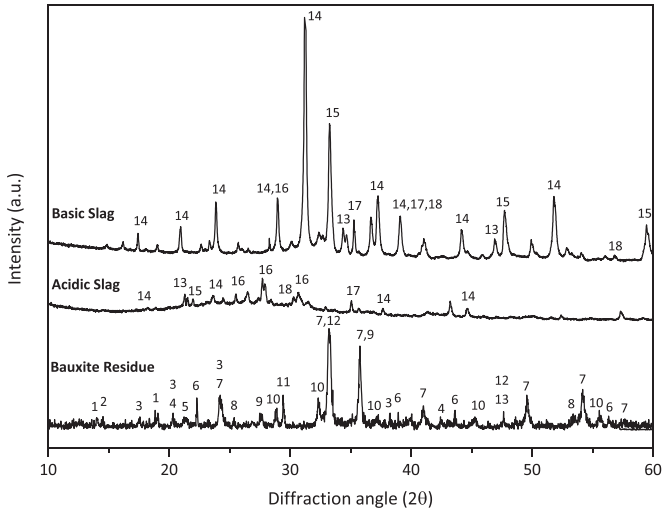

Fig. 2. XRD Diffractograms of acidic and basic slags (1: $2CaO{\cdot}Al_2O_3{\cdot}SiO_2$, 2: $CaTiO_3$, 3: $2CaO{\cdot}SiO_2$, 4: $CaO{\cdot}SiO_2$, 5: $3CaO{\cdot}SiO_2$, 6: $CaO{\cdot}Al_2O_3$).

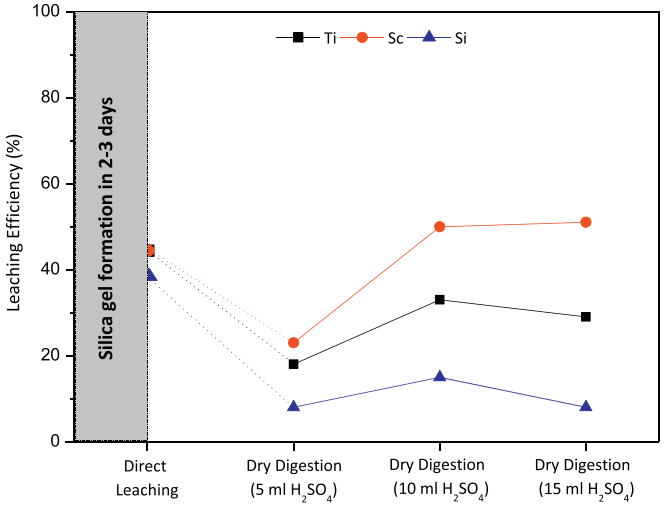

Fig. 3. Leaching efficiencies of Sc, Ti and Si from red mud by dry digestion with various acid additions at the end of 1 h.

slag are replaced with poorly crystalline phases and a high content of amorphous content due to high amount of SiO_2 in the acidic slag. In both slags, different stoichiometry of Ca-Al-Si oxides were observed. Moreover, due to the high amount of Ca and also better crystallinity, higher amount of well-defined perovskite are observed in the basic slag which may affect leaching behaviour of Ti, as well as Sc, which exist in the Al and Ti based phases.

Both slags and as a reference material, red mud, were first treated by direct leaching, and the tendency to form silica gel of pregnant leaching solutions was observed, as given in Table 2.

As expected, increasing the Si content of the solid shortened the gelation time, which necessitates the application of the dry digestion method for enhanced recoveries and processable pregnant leaching solutions.

After establishing the necessity of dry digestion for slag treatment, dry digestion was first applied on red mud. In order to have a direct comparison, the acid (15 ml) to solid material (13 g) ratio (a/s: 1.15) was kept constant with direct leaching conditions and then acid amount varied to 10 (a/s: 0.77)and 5 ml (a/s: 0.38) (keeping solid amount constant and decreasing acid to solid ratio) to find the optimum acid requirement in terms of leaching efficiency and minimized acid consumption. Leaching efficiencies for Sc, Ti and Si can be found in Fig. 3.

In the case of direct leaching, Sc and Ti extraction efficiencies were around 45 and 50%, respectively. However, here it is important to note that, there was also an important amount of dissolved Si (40%) in the leachate, which resulted in silica gel formation within 2–3 days as given in Table 2. Application of dry digestion with all acid amounts (5 mL, 10 mL, 15 ml) resulted in the suppression of Ti and Si dissolution, which indicates a solid residue enriched in terms of SiO_2 and Ti-Oxide. In the case of Sc, an optimum acid use (15 mL) increased Sc leaching efficiency to 50%. It is reported previously that Sc is found in hematite in the red mud, where the main phase is a mixed oxide of Fe Ca Al and Si (Alkan et al., 2017a; Vind et al., 2018a,b). When concentrated H_2SO_4 reacts with that mixed oxide, the rapid formation of gypsum and silica may result in boundary effects and hinder further leaching. However, there are also free hematite particles revealed in the red mud that are not embedded in the main mixed oxide, which provide easily leachable Sc. Increased acid amounts pronounce the formation of that surrounding gypsum and silica layer that decreases leaching efficiencies. These findings on red mud imply that the dry digestion process with an optimized acid concentration may yield in selective and enhanced Sc leaching without gelation problem and a mineral residue enriched in terms of Ti-ox, which may be used in further cement applications.

Table 2
Gelation times of red mud and slags.

	Red mud	Basic slag	Acidic slag
Gelation time	2–3 days	2–3 h	Rapid gelation

Red mud mineral distribution and their associations have been studied extensively in our previous study, which helps us to understand leaching mechanism. After removal of a substantial portion of the Fe and due to the chemical additives and high temperature in the EAF furnace treatment, the starting materials, acidic and basic slags should exhibit a completely different minerology. In order to explain the leaching mechanism of desired metals and propose a leaching model, it is crucial to understand the mineralogy and the phases of the initial materials. Therefore, acidic slag and basic slag were analysed by QEMSCAN; especially to reveal Ti entrapments as given in Fig. 4. Since Sc is present just in ppm level, it was not possible to monitor its hosting minerals by QEMSCAN.

Fig. 4a and b reveal the distribution of the main Ti phase within the acidic and basic slags. Due to high CaO addition in the basic slag, Ti is crystallized in a perovskite phase as indicated with orange particles as can be seen in Fig. 4a, while it exists as Ti-oxide in the acidic slag. In both slags, an important amount of Ti including mineral is surrounded with the complex oxides. Cuspidine (Ca—Al— oxide) and Si enriched gehlenite (Ca Al Si oxide) were revealed by QEMSCAN as the main minerals that encapsulate titanium in the basic and acidic slag; respectively. Another distinction between acidic and basic slag is the particulate size. Coarser particles of basic slag was replaced by finer particles of acidic slag, which is directly related to the lack of crystal formation and growth in the case of highly amorphous nature of acidic slag. Moreover, the particulate mapping of both slags uncover that a significant amount of perovskite is located at the surface of cuspidine particles, whereas Ti-oxide is found mainly in the inner parts of Si enriched gehlenite of acidic slag. Beyond mineralogical mapping, QEMSCAN also enabled to analye particle size distribution of three starting materials as given in Fig. 5.

Although all slags were milled with an aim to have particles smaller than 90 µm, there were some agglomerations observed in some particulates which resulted in size bigger than 100 µm. But ESD revealed that both samples exhibit mainly smaller than 63 µm. This analysis highlight acidic slag exhibit relatively bigger particle size, which may promote the surrounding barrier effect.

After understanding the differences between the acidic and basic slags in terms of mineralogy, they were subjected to dry digestion in a

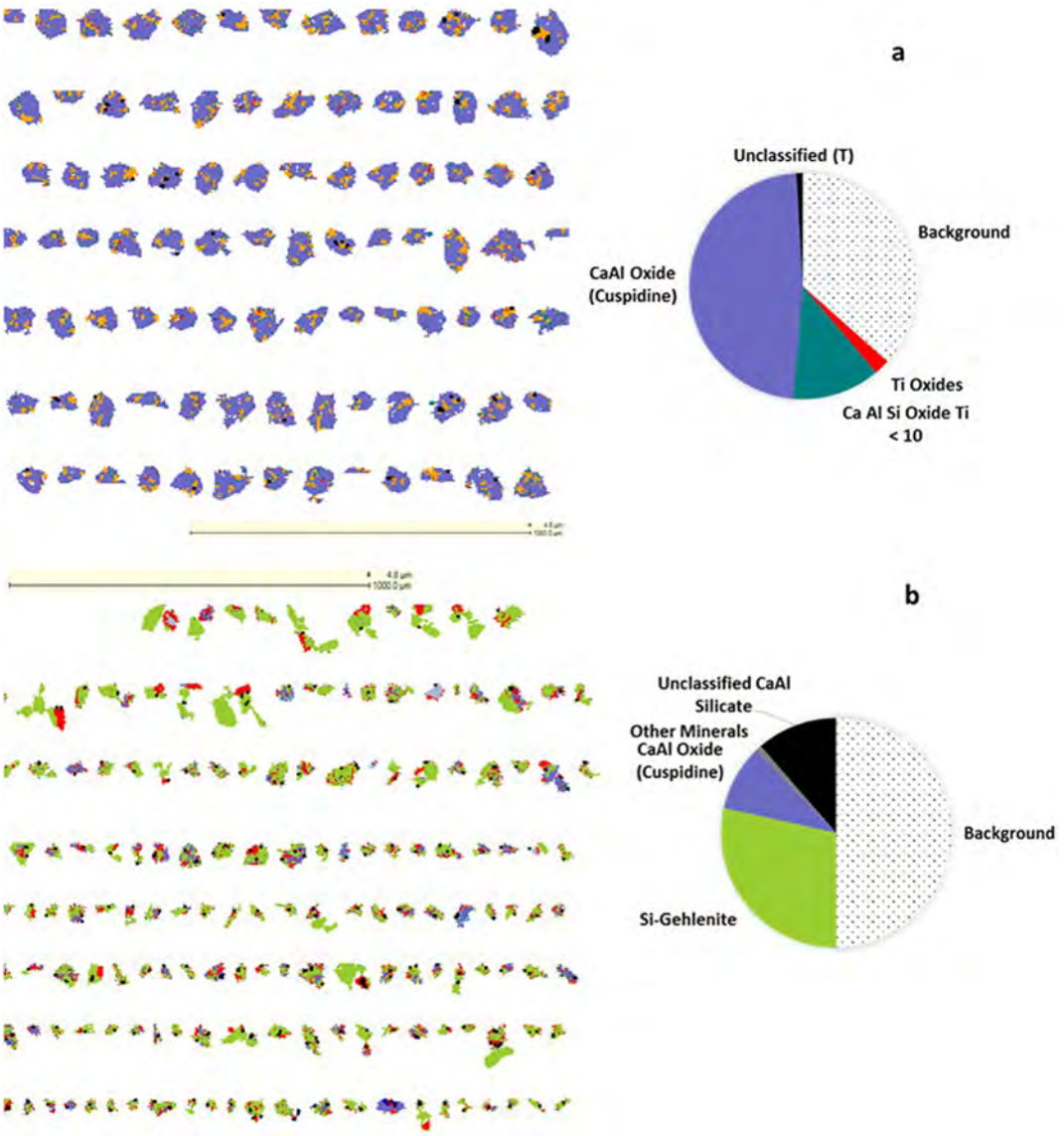

Fig. 4. QEMSCAN revealing Ti-ox entrapment in (a) acidic slag, and perovskite entrapment in (b) basic slag.

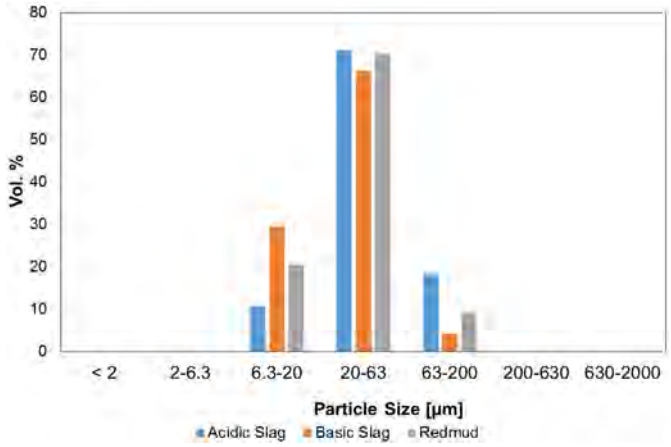

Fig. 5. Equivalent sphere diameter (ESD) of acidic slag, basic slag and red mud, evaluated by QEMSCAN.

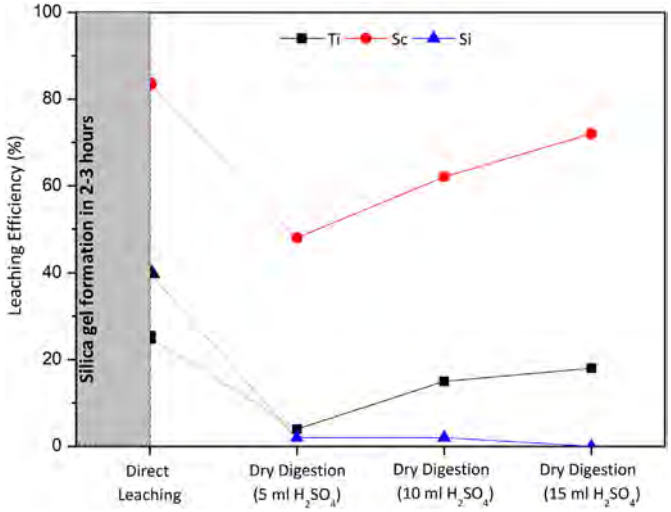

Fig. 6. Leaching efficiencies of Sc, Ti and Si from basic slag by dry digestion with various acid additions at the end of 1 h.

comparative manner to the direct leaching. 4 wt% of the SiO_2 content of red mud is enriched in the slags after substantial Fe removal, which increases the gelation risk dramatically. In order to assess the limits of dry digestion process, acidic and basic slags were examined in identical conditions as in the red mud leaching. Fig. 6 reveals leaching efficiencies of Sc, Ti and Si from basic slag.

In the case of direct leaching with sulfuric acid, 84% of Sc recovery was achieved. However, as listed in Table 2, just within 2 h, gelation of PLS occurred, which could not be proceeded to further recovery steps. However, with the application of dry digestion, independent of the amount of acid to solid ratio, silica dissolution was successfully supressed and no gelation was observed. These results prove the strength of dry digestion on basic slag in terms of inhibition of gelation.

It is also important to note that the removal of Fe and enrichment of slag in terms of Ti content did not enhance Ti leaching efficiency. Ti leaching efficiency of 50% from red mud was decreased to 25%, in the case of basic slag by direct leaching. With the application of dry digestion, this value is even more lowered, as can be seen in Fig. 6. As revealed by XRD and QEMSCAN analyses, the formation of crystalline and stable perovskite may be the reason of this inhibition effect. Most probably, most of the dissolved Ti was provided by perovskite particles located near to the surface as revealed in Fig. 4a.

Moreover, due to the high CaO (~43 wt%) content of the basic slag, H_2SO_4 in the system is mainly used up for gypsum formation, which has fast reaction kinetics, and hence increases the need for additional H_2SO_4 to dissolve other oxides. Therefore, slight increases in the leaching efficiencies were observed with increasing acid concentration. Although dry digestion on basic slag increased the selectivity of Sc leaching against Ti, it also resulted in a slight decrease in Sc leaching efficiency to 70% when compared with direct leaching. As the host of Sc in red mud was removed by EAF treatment, Sc is hosted by CaAl-oxide phases. Therefore, with higher Ca and Al dissolution, Sc recovery is also favoured. However, as a gypsum layer starts to form at the surface of the particles it behaves as a barrier which suppresses further leaching of Sc. Moreover, it is known that the minor host for Sc in these slags are Ti including phases following Al oxides. Since a certain amount of Ti-oxide remains undissolved, this may also result in relatively lower Sc leaching efficiency.

After basic slag, acidic slag, which is an extreme case with 38% SiO_2, was examined in the same manner. Leaching efficiencies are given in Figs. 6 and 7.

Due to the very high SiO_2 content, immediate silica gel formation took place in the case of direct leaching. Application of dry digestion on even SiO_2 enriched slag (~40 wt%) prevented silica gelation and

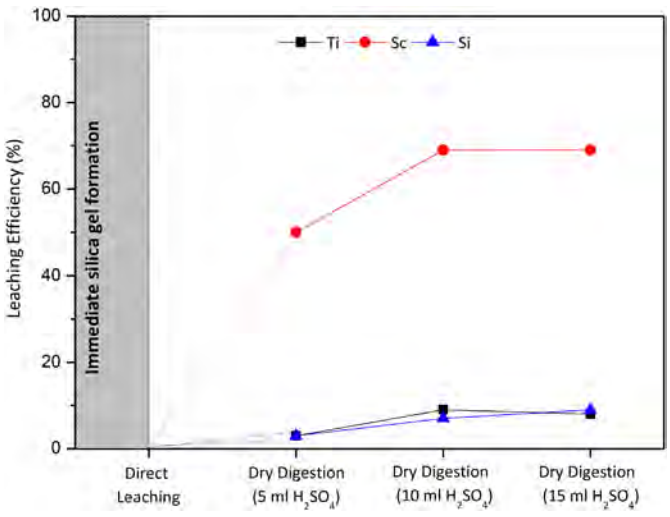

Fig. 7. Leaching efficiencies of Sc, Ti and Si from acidic slag by dry digestion with various acid additions at the end of 1 h.

proved the strength of the method against gel formation problem. In parallel with basic slag, a further suppression of Ti-oxide dissolution was observed in the acidic slag to values even lower than 10%. Dry digestion with 15 mL acid concentration on acidic slag exhibited the most selective against Ti and the highest Sc leaching efficiency (~70%). The amorphosity of the acidic slag was found out to be extremely high as a result of high glass former Si amount in the slag, as given in the XRD analyses in Fig. 2, which increases the acid resistance and therefore suppress Ti-oxide dissolution substantially. Furthermore, a high amount of perovskite particles are located at the surface of cuspidine, as revealed in Fig. 4a, may be responsible for relatively higher Ti dissolution in the basic slag, when compared with the acidic slag (> 10%). Moreover, the leading phase was a Si enriched Ca Al oxide, and the relatively bigger particle size of the acidic slag as given in Fig. 5, may enhance the boundary effect, where concentrated acid results in SiO_2 and gypsum precipitation, again preventing the leachate to reach inner parts of the slag.

In order to understand the dry digestion mechanism better, solid residue of basic slag after treatment was analysed by QEMSCAN, which is given in Fig. 8.

This QEMSCAN analysis proves that an unreacted core is surrounded by a gypsum layer, which acts like a diffusion barrier and prevents further interaction between the concentrated acid and the slag. Since during the dry digestion process precipitation of insoluble silica takes place owing to increased ionic strengths, similar surrounding layer but consisting of SiO_2 instead of gypsum may form in the case of acidic slag. This may be the reason of dramatically suppressed leaching of Ti and the enrichment of solid residue in terms of TiO_2 as most of the Ti phases are surrounded by Si enriched gehlenite phase.

Using these leaching efficiency data and mineralogical information of starting and end materials, a comparative reaction model was proposed for the dry digestion of red mud, acidic and basic slag as given in Fig. 9.

Different mineralogy and degrees of crystallinity of the starting materials lead to various leaching efficiencies of Sc and selectivity of Sc over Ti. In all cases, as a result of the precipitation of Si as SiO_2, silica gel formation was successfully prevented. Since reaction initiates from the surface of the particles and in the case of dry digestion, a very limited amount of concentrated acid is used, a boundary effect occured in all systems. Depending on the leading mineral, the leachability of Sc and Ti were varied as represented in Fig. 9. While formation of gypsum, rhomboclase and silica in the red mud was the major reason why acid could not penetrate the core of the particles and transform the targeted metals into soluble sulphates, in the case of slags, particle size and distribution has one of the most important roles. Furthermore, leaching behaviour of each slag varied depending on the fluxing agent, CaO and SiO_2, yielding either gypsum rich or silica rich shield around the particles.

4. Conclusion

In this study, red mud and two different Fe depleted slags with different chemistries produced from red mud by smelting were exposed to dry digestion with the intention of recovering Sc selectively by supressing Ti and Si dissolution. The major problem of using traditional leaching methods while dealing with Si enriched materials is the formation of silica gel, and this was completely supressed in all three cases when the dry digestion method was implemented. It was found that when compared with direct leaching conditions, there is a certain suppression of the leaching efficiencies due to rapid reaction kinetics and formation of sulphates as a surrounding layer, which prevents acid to penetrate into the particle core. However, this suppression was more pronounced in the case of acidic slag where Ti (< 10%) and Si (< 3%) were successfully supressed, which favours the selective Sc leaching with an efficiency of 70%. Dry digestion was thus found to be a

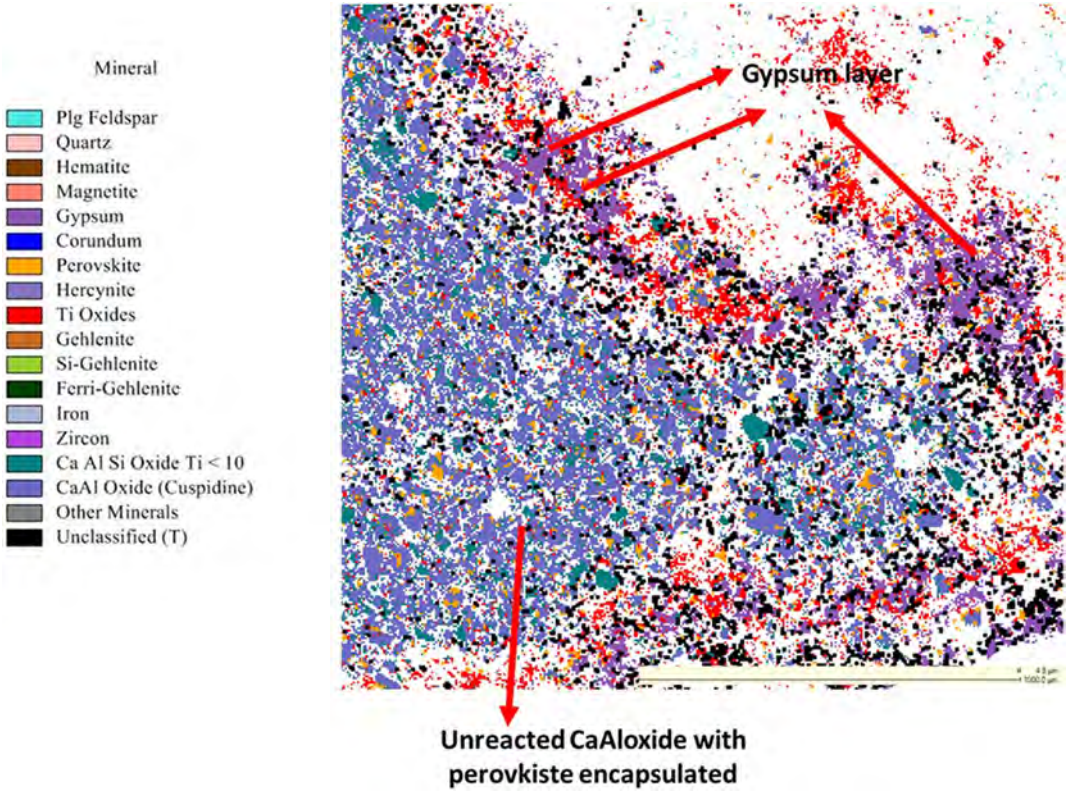

Fig. 8. QEMSCAN mineralogical mapping of dry digestion residue of basic slag.

promising method to treat Fe depleted slags, clearly surpassing the direct extraction of Sc from red mud, where conventional routes are unsuitable because of the Si gel formation.

Although the equipment to handle such a process should be highly resistant to corrosion due to the use of concentrated acids, the acid consumption and duration of operation are lower as well as handling of the process is easier than conventional leaching methods applied to red mud.

5. Acknowledgements

The research leading to these results has received funding from the European Community's Horizon 2020 Programme ([H2020/2014–2019]) under Grant Agreement No. 636876 (MSCA-ETN REDMUD). This publication reflects only the author's view, exempting the Community from any liability. Project website: http://www.etn.redmud.org.

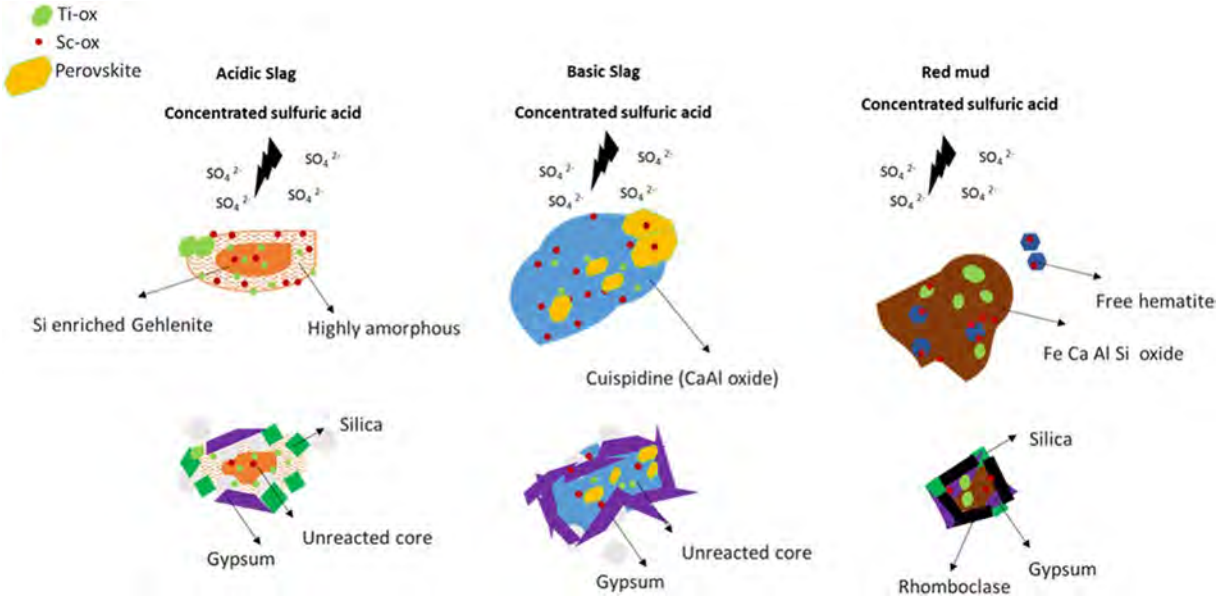

Fig. 9. Comparative dry digestion mechanisms of red mud, acidic and basic slag.

Appendix A. Supplementary data

Supplementary data to this article can be found online at https://doi.org/10.1016/j.hydromet.2019.03.008.

References

Alkan, G., Schier, C., Gronen, L., Stopic, S., Friedrich, B., 2017a. A mineralogical assessment on residues after acidic leaching of bauxite residue (red mud) for titanium recovery. Metals 7 (11), 458.

Alkan, G., Xakalashe, B., Yagmurlu, B., Kaussen, F., Friedrich, B., 2017b. Conditioning of red mud for subsequent titanium and scandium recovery–a conceptual design study. World of metallurgy–ERZMETALL 70 (2), 5–12.

Alkan, G., et al., 2018. Novel approach for enhanced scandium and titanium leaching efficiency from bauxite residue with suppressed silica gel formation. Sci. Rep. 8 (1), 5676.

Avdibegović, D., et al., 2018. Combined multi-step precipitation and supported ionic liquid phase chromatography for the recovery of rare earths from leach solutions of bauxite residues. Hydrometallurgy 180, 229–235.

Borra, C.R., Pontikes, Y., Binnemans, K., Van Gerven, T., 2015. Leaching of rare earths from bauxite residue (red mud). Miner. Eng. 76, 20–27.

European Commission, 2017. Study on the review of the list of Critical Raw Materials: executive summary. In: Directorate-General for Internal Market, Industry, Entrepreneurship and SMEs.

Feuling, R.J., 1991. In: Patents, U. (Ed.), Recovery of scandium, yttrium and lanthanides from titanium ore.

Haslam, M., 1999. An investigation into the feasibility of extracting scandium from nickel laterite ores. In: Proceeding of ALTA 1999 Nickel/Cobalt Pressure Leaching & Hydrometallurgy Forum. ALTA Metallurgical Services.

Heilbronner, R., Barrett, S., 2014. Crystal orientation and interference color. In: Image Analysis in Earth Sciences. Springer, pp. 413–438.

Kaya, Ş., Dittrich, C., Stopic, S., Friedrich, B., 2017. Concentration and separation of scandium from Ni laterite ore processing streams. Metals 7 (12), 557.

Ma, Y., Stopic, S., Gronen, L., Friedrich, B., 2018. Recovery of Zr, Hf, Nb from eudialyte residue by sulfuric acid dry digestion and water leaching with H2O2 as a promoter. Hydrometallurgy 181, 206–214.

Marquis, E., Seidman, D., 2001. Nanoscale structural evolution of Al 3 Sc precipitates in Al (Sc) alloys. Acta Mater. 49 (11), 1909–1919.

Narayanan, R.P., Kazantzis, N.K., Emmert, M.H., 2017. Selective Process Steps for the Recovery of Scandium from Jamaican Bauxite Residue (Red Mud). ACS Sustainable Chemistry & Engineering.

Paramguru, R., Rath, P., Misra, V., 2004. Trends in red mud utilization–a review. Miner. Proc. Extract. Metall. Rev. 26 (1), 1–29.

Queneau, P.B., Berthold, C.E., 1986. Silica in hydrometallurgy: an overview. Can. Metall. Q. 25 (3), 201–209.

Rivera, R.M., Ulenaers, B., Ounoughene, G., Binnemans, K., Van Gerven, T., 2018. Extraction of rare earths from bauxite residue (red mud) by dry digestion followed by water leaching. Miner. Eng. 119, 82–92. https://doi.org/10.1016/j.mineng.2018.01.023.

Røyset, J., Ryum, N., 2005. Scandium in aluminium alloys. Int. Mater. Rev. 50 (1), 19–44.

Sadri, F., Nazari, A.M., Ghahreman, A., 2017. A review on the cracking, baking and leaching processes of rare earth element concentrates. J. Rare Earths 35 (8), 739–752.

Safarzadeh, M., Moats, M., Miller, J., 2012a. Evaluation of sulfuric acid baking and leaching of enargite concentrates. Miner. Metall. Proc. 29 (2).

Safarzadeh, M.S., Moats, M.S., Miller, J.D., 2012b. Acid bake-leach process for the treatment of enargite concentrates. Hydrometallurgy 119, 30–39.

Vind, J., Alexandri, A., Vassiliadou, V., Panias, D., 2018a. Distribution of selected trace elements in the Bayer process. Metals 8 (5), 327.

Vind, J., et al., 2018b. Modes of occurrences of scandium in Greek bauxite and bauxite residue. Miner. Eng. 123, 35–48.

Voßenkaul, D., Birich, A., Müller, N., Stoltz, N., Friedrich, B., 2017. Hydrometallurgical processing of eudialyte bearing concentrates to recover rare earth elements via low-temperature dry digestion to prevent the silica gel formation. J. Sust. Metall. 3 (1), 79–89.

Yagmurlu, B., Dittrich, C., Friedrich, B., 2017. Precipitation trends of scandium in synthetic red mud solutions with different precipitation agents. J. Sust. Metall. 3 (1), 90–98.

Yamamoto, O., 2000. Solid oxide fuel cells: fundamental aspects and prospects. Electrochim. Acta 45 (15), 2423–2435.